

Dimerization of NO and transformation to N₂O on Ge(100)

B. M. Davies* and J. H. Craig, Jr.

Department of Physics, Bradley University, Peoria, IL 61625

*Corresponding author. Phone: 309-677-3305 Fax: 309-677-2999, e-mail: bdavies@bradley.edu

Abstract

Temperature-programmed desorption studies of submonolayer coverages of nitric oxide (NO) on a Ge(100) (2x1) surface have previously determined the non-dissociative nature of the adsorption of NO on Ge(100) at 110 K. Subsequent electron bombardment results in electron-stimulated desorption of N₂O and N₂ at that temperature, without heating, which is attributed to the formation of NO dimers on the cold surface. This conclusion is supported by studies of adsorbed layers of N₂O, which is adsorbed at least partly non-dissociatively, and which yields little desorption of the parent N₂O molecule when bombarded with electrons.

Keywords: Adsorption; Germanium; Nitric oxide; Nitrous oxide; Electron Stimulated Desorption (ESD); Temperature Programmed Desorption (TPD)

PACS codes: 79.20.L

1. Introduction

Reactions of nitric oxide (NO) and nitrous oxide (N_2O) on various substrates have been of interest for a variety of reasons. The reduction of harmful emission of nitrogen oxides from automotive engines has motivated studies of adsorption on metal surfaces, as well as metal oxide surfaces. Of particular interest has been the question of whether it is possible to form an N-N bond and subsequent production of N_2 or N_2O without the dissociation of NO. The usual mechanism is proposed to require a dissociation event, which yields an adsorbed N which then reacts with another adsorbed N to form N_2 or with NO to form N_2O . An alternate mechanism, not requiring dissociation, is the formation of NO dimers (or dinitrosyl intermediates) with formula $(\text{NO})_2$ which then decompose into N_2O and O. A better understanding of this alternate mechanism may allow the design of catalysts which require lower temperature or are less expensive.

The formation of dimers of NO has been reported in numerous publications, in both the gas phase [1] and condensed phase [2]. The structure of the gas phase dimer is still subject to debate [3], but a likely structure is shown in Fig. 1, along with a potential bonding orientation on a surface. Other structures are possible, in particular a trans configuration with a zig-zag geometry. In these various geometries, the topology would be described as O-N-N-O, with the nitrogens bonding together, and the oxygens not bonded to each other but only bonded to the nitrogens.

On metals the formation of dimers and production of N_2O is linked to the non-dissociative nature of NO adsorption on selected surfaces. On Cu(100) the formation of dimers occurs below 60 K with subsequent desorption of N_2O upon heating above 60 K [4]. On Ag(111) the adsorption is both dissociative and molecular [5-9], and dimer

formation occurs at very low temperatures (40 to 60 K) with N₂O desorption at 70 to 90 K [6-8]. Various Pt surfaces have been studied and show contrasting behavior. No dimer formation was suggested in a study of Pt(100) [10]. On Pt(111) the adsorbed NO molecule induces a significant change in the electronic structure of the substrate [11], and through-substrate effects are postulated to describe certain features of vibrational spectra for multi-site adsorption [12], but no dimers were postulated in either study. By depositing a layer of Ag on the Pt(111) surface, dimers are formed (as might be expected for a Ag surface) in addition to new species [13]. In contrast, studies of the lateral interactions between NO molecules on Pt(100) have led to the proposal of polymeric (NO)_x chains on the surface at high coverage [14-15]. Such contrasting behaviors have led to studies of surface modification as a tool for altering the energetics of the reaction. On W(100), for example, NO adsorbs dissociatively, but by adding well-ordered, thermally stable overlayers of oxygen (p(2x2)-O and p(2x1)-O), the dissociation is suppressed and the yield of N₂O and N₂ is enhanced, proceeding via a nondissociative reaction pathway involving a proposed NO dimer as the reaction intermediate [16]. Additional details of the effect of surface modification on this process were obtained for a carbon-covered surface, W(100)-p(5x1)-C, also involving inhibition of NO dissociation and an NO dimer intermediate [17]. Recent theoretical work [18] has clarified the energetics of reaction pathways through these dimer intermediates, by contrasting the behavior of NO on Cu(111) and Pt(111). According to this study, both substrates adsorb NO non-dissociatively, but only on Cu(111) do NO dimers form, and only Cu(111) has the ability to transform NO directly into N₂ or N₂O.

An alternative mechanism involves dinitrosyl groups, with two NO molecules bound to a common site, for example, on Mo(110) [19]. Oxygen may stabilize the nitrosyl group on Mo(110) [20], whereas oxygen defects may produce the dinitrosyl group on highly oxidized Mo(110) [21]. Contrasting behavior between the dinitrosyl and dimer are seen on this same surface [22]. The dinitrosyl group may also be present on supported iron oxides [23]. These systems are evidently complex, and recent theoretical work has focused on density-functional theory studies of simple model systems, such as Cu-Dinitrosyl [24], NiNO, Ni₂NO and Ni₂(NO)₂ [25], and Pd and Pt nitrosyls and dinitrosyls [26]. Similar theoretical studies have elucidated the mechanism of NO adsorption on MgO [27-28], and have led to recent work [29] which concludes that NO adsorbs in pairs consisting of a Lewis acid NO and a Lewis base NO, with significant electron transfer between the two, and a strong stabilizing electrostatic interaction. Thus a third mechanism is possible due to the amphoteric nature of the NO radical.

In this work, we study the production of N₂O from NO adsorbed on a semiconducting substrate, germanium, and present evidence that formation of NO pairs (most likely dimers) occurs at low temperature. Our previous work investigated the formation of oxynitrides using NO as a precursor on germanium [30], or on silicon substrates [31]. Reaction products were detected using temperature-programmed desorption (TPD) of neutrals and electron-stimulated desorption (ESD) of ions and neutrals. Certain results for the desorption products of adsorbed NO were puzzling until we also investigated the adsorption of N₂O on Ge(100), with its desorption products, which leads us to propose the relevance of NO dimerization in the ESD of adsorbed NO layers. Taken with the cited literature suggesting the pairing of NO on metals and on insulators, this result for a

semiconducting substrate indicates that dimerization of NO may occur for a wide variety of substrates.

2. Experimental Details

This study used an ultra-high vacuum system which has been described in detail elsewhere [32, 33]. Additional details and drawings may be found in several Ph.D. dissertations [34-36]. New aspects of the experimental procedure used in this study are described here.

The Ge(100) sample was cleaned *in situ* by a thermal anneal in a vacuum of 2×10^{-10} torr. Typical temperature ramp rates were 3 K/s for heating and 2 K/s for cooling, with a 2 minute dwell at between 800 K and 870 K, as measured by an infrared optical pyrometer (Raytek Thermalert 30 with sensing head RAYSHMTCF2). Upon advice from the manufacturer, we used an emissivity setting of 0.8 for the wavelength used by the pyrometer (3.9 μm). This procedure resulted in the appearance of a sharp 2×1 LEED pattern at low temperature. An occasional Argon ion sputter was used to remove nitride from the surface, as determined by Auger spectroscopy.

TPD data was obtained at a heating rate of 3 K/s, as measured by a thermocouple attached to the back of a silicon-tantalum-silicon sandwich which served as the heater and mount for the Ge sample. Electron irradiation was from a Kimball Physics electron gun (model EFG-7) at beam energy 600 eV and current density $1.2 \mu\text{A}/\text{cm}^2$, incident on the sample at an angle of 60° with respect to the sample normal.

Gas dosing through a tubular array doser located 1 cm from the sample was quantified by measuring the pressure with an ionization gauge. A voltage output from the ionization gauge controller was then measured and integrated using a PC. The exposure is given in Langmuir (L), which is equal to 10^{-6} Torr-sec. The actual exposure of the sample surface from the tubular array doser is greater than a conventional exposure done by backfilling the chamber, and we estimate an amplification on the order of 10.

3. Results and discussion

TPD spectra for NO dosed onto Ge(100) at 110 K have been presented in previous publications [30, 37]. These show that as the NO dose increases, the desorption of mass 30 (NO molecules) increases, producing a weak desorption peak at about 220 K as the dose reaches 0.7 L, which is consistent with previous results indicating mostly non-dissociative adsorption [30]. Likewise, the desorption of mass 28 (N_2) has a peak at about 190 K, particularly at the higher 0.7 L dose. In the cracking pattern for NO gas in our mass spectrometer, which was reported in a recent dissertation [36], the mass 28 peak is less than 5% of the height of the mass 30 peak, so we conclude that this peak is due to desorption of N_2 from the surface. The absence of a mass 28 peak in the cracking pattern for NO is also reported in earlier work [38] using a different spectrometer. This desorption peak for nitrogen molecules indicates that N-N bonds are being formed at fairly low temperatures, since these bonds will not be present in the case of adsorption of NO as intact molecules (i.e., as monomers).

Similar desorption behavior occurs for N_2O dosed onto Ge(100), as shown in Fig. 2, except that all three masses, mass 30, mass 28, and mass 44 (the parent molecule N_2O),

display desorption peaks occurring at slightly lower temperature, about 140 K. Some of the intensity of the mass 28 and 30 peaks is due to cracking of N_2O in the mass spectrometer; as indicated in previous work [38] the mass 30 peak due to cracking is about 31 % of the mass 44 peak, and the mass 28 peak is about 11 % of the mass 44 peak. The TPD curves of Fig. 2 show a mass 28 peak significantly larger than both the mass 44 and mass 30 peaks, and a mass 30 peak comparable to the mass 44 peak, and hence we conclude that both mass 28 and mass 30 are desorbing from the surface. The desorption of mass 28 and of mass 30 could indicate the direct dissociation of the parent molecule, N_2O , into N_2 and NO . In this case, the production of N_2 would be occurring without the formation of new bonds between nitrogen atoms, as might be occurring in the case of NO adsorption.

Electron irradiation of the adsorbate-covered $\text{Ge}(100)$ surface produces desorption of neutrals, and we find that useful information can be obtained by monitoring this desorption during irradiation. Fig. 3 shows a series of desorption curves obtained previously [37] during a 2 minute irradiation of the NO dosed $\text{Ge}(100)$. The electron gun was gated on at a time of about 30 s, and kept on until 2 min 30 s, when it was gated off. The top set of curves corresponds to mass 30 desorption for increasing doses from 0.15 L to 0.7 L, with the curves offset vertically for clarity. At low doses, the desorption is approximately constant during this 2 min period, but for a dose of about 0.5 L and above, the NO desorption displays a peak during the first 15 seconds of irradiation. [Also note that the sloped background on the mass 30 data for 0.7 L is due to a steadily decreasing background partial pressure of residual NO from the dosing process. It was difficult to maintain a constant time period between the end of dosing and the beginning of data

collection, and so it varied from about 2 to 5 minutes delay.] The second set of curves in Fig. 3 reveal similar behavior for mass 28, except that there is no sloping background of N_2 partial pressure after the dosing. In particular, note the existence of very similar behavior in the 15 s peak at the beginning of irradiation for the higher doses. This behavior suggests the presence of a second species of NO (or additional products) on the surface for doses higher than about 0.5 L. Mass 44 desorption, shown in the third set of curves, displays an initial rise to an approximately constant rate, even for higher doses, in contrast to the presence of the initial 15 s peak in the mass 30 and mass 28 data. This suggests that the mass 44 desorption is associated with the species of NO or related products that are present at the low doses, and not with the species of NO (or products) that contributes to the 15 s peak at higher doses.

As mentioned in our previous work on low coverages [37], it is difficult to explain the near simultaneous thermal desorption of mass 44 and mass 28, in addition to the expected mass 30, from an initial coverage of NO at such low temperatures without postulating the existence of dimers on the surface, which would produce the N-N bonds needed to get mass 44 or mass 28 products. The TPD results shown in reference [37] even suggest that it is about as likely for such dimers to decompose into N_2 or N_2O at low temperature as it is for them to desorb as single NO molecules. In particular, the desorption curves for mass 28 and 30 are almost identical.

Additional evidence for dimer formation is provided by the ESD data, which indicates that mass 44 is produced by electron bombardment. This suggests several possibilities: electron-induced reactions between NO and N on the surface, decomposition of a dimer of topology ONNO, or direct electron-induced desorption of

N₂O molecules which are present on the surface just after dosing with NO at 110 K. We believe that the first possibility is unlikely to produce such a large signal, and will show that the third possibility does not occur by studying the adsorption of N₂O.

To confirm dimer formation, additional work was done on adsorbed layers of N₂O on Ge(100). Fig. 4 shows ESD results for a dose of 0.5 L of N₂O, followed by 10 min of electron irradiation starting at 30 seconds. Immediately after the ESD run, a TPD run was initiated to investigate what remained on the surface. As seen in Fig. 5, the N₂O peak has been virtually eliminated by the electron bombardment (compare with Fig. 2 for unirradiated N₂O doses). Similar results were obtained for higher doses, except that more electron bombardment was required to eliminate the N₂O TPD peak. The low yield of mass 44 in these ESD curves indicates that N₂O is not directly desorbed by electron irradiation from an N₂O layer. Hence, in the case of NO layers, the yield of mass 44 in the ESD curves must not be due to the transformation of NO into N₂O during the adsorption. The surface was too cold to desorb the N₂O by thermal means, and the results of Fig. 4 show that electrons would not desorb the adsorbed N₂O as an intact molecule. Instead, we conclude that the N₂O product is produced by the electron-induced decomposition of a dimer having topology ONNO. The energy of an incident electron then breaks the ON bond, resulting in the desorption of NNO and leaving O on the surface. [At this point, we have not performed calculations to suggest an adsorption geometry for the NO dimers. Given the recent increase in cited work regarding dimer formation on metals and insulators, a theoretical study of NO dimer formation on this semiconducting substrate may be of value.]

4. Conclusions

The adsorption of submonolayer coverages of NO on a Ge(100) surface at low temperatures was studied by TPD and by electron stimulated desorption. TPD peaks at low temperature indicate the primarily non-dissociative nature of the adsorption. ESD of neutrals suggests the presence of a second species of NO on the surface for doses higher than about 0.5 L. The TPD results also suggest the presence of NO dimers on the surface for low coverage, which then decompose to produce desorption of N₂O and N₂ at low temperatures. Additional evidence for dimer formation is provided by ESD studies of adsorbed NO and also adsorbed N₂O, which suggest the presence of dimers rather than N₂O on the NO-dosed surface.

References

- [1] S. G. Kukolich, *J. Am. Chem. Soc.* 104 (1982) 4715.
- [2] E. M. Nour, L.-H. Chen, M. M. Strube, and J. Laane, *J. Phys. Chem.* 88 (1984) 756.
- [3] J. K. Park and H. Sun, *Bull. Korean Chem. Soc.* 20 (1999) 1399.
- [4] C. M. Kim, C-W. Yi, and D. W. Goodman, *J. Phys. Chem. B* 106 (2002) 7065.
- [5] S. K. So, R. Franchy, and W. Ho, *J. Chem. Phys.* 91 (1989) 5701.
- [6] W. A. Brown, P. Gardner, M. Perez Jigato, and D. A. King, *J. Chem. Phys.* 102 (1995) 7277.
- [7] W. A. Brown, P. Gardner, and D. A. King, *J. Phys. Chem.* 99 (1995) 7065.
- [8] M. Perez Jigato, D. A. King, and A. Yoshimori, *Chem. Phys. Lett.* 300 (1999) 639.
- [9] R. T. Kidd, D. Lennon, and S. R. Meech, *J. Phys. Chem. B* 103 (1999) 7480.
- [10] E. D. L. Rienks, J. W. Bakker, A. Baraldi, S. A. C. Carabineiro, S. Lizzit, C. J. Weststrate, and B. E. Nieuwenhuys, *Surf. Sci.* 516 (2002) 109.
- [11] Q. Ge and D. A. King, *Chem. Phys. Lett.* 285 (1998) 15.
- [12] H. Aizawa, Y. Morikawa, S. Tsuneyuki, K. Fukutani, and T. Ohno, *Surf. Sci.* 514 (2002) 394.
- [13] T. Itoyama, M. Wilde, M. Matsumoto, T. Okano, and K. Fukutani, *Surf. Sci.* 493 (2001) 84.
- [14] W. A. Brown, Q. Ge, R. K. Sharma, and D. A. King, *Chem. Phys. Lett.* 299 (1999) 253.

- [15] Q. Ge, W. A. Brown, R. K. Sharma, and D. A. King, *J. Chem. Phys.* 110 (1999) 12082.
- [16] E. K. Baldwin and C. M. Friend, *J. Phys. Chem.* 89 (1985) 2576.
- [17] E. K. Baldwin and C. M. Friend, *J. Phys. Chem.* 91 (1987) 3821.
- [18] A. Bogicevic and K. C. Hass, *Surf. Sci.* 506 (2002) L237.
- [19] K. T. Queeney and C. M. Friend, *J. Chem. Phys.* 107 (1997) 6432.
- [20] K. T. Queeney and C. M. Friend, *J. Phys. Chem. B* 102 (1998) 9251.
- [21] F. C. Nart and C. M. Friend, *J. Phys. Chem. B* 105 (2001) 2773.
- [22] K. T. Queeney, S. Pang, and C. M. Friend, *J. Chem. Phys.* 109 (1998) 8058.
- [23] D. G. Rethwisch and J. A. Dumesic, *J. Phys. Chem.* 90 (1986) 1625.
- [24] R. Ramprasad, K. C. Hass, W. F. Schneider, and J. B. Adams, *J. Phys. Chem. B* 101 (1997) 6903.
- [25] H. A. Duarte and D. R. Salahub, *J. Phys. Chem. B* 101 (1997) 7464.
- [26] A. Citra and L. Andrews, *J. Phys. Chem. A* 104 (2000) 8160.
- [27] X. Lu, X. Xu, N. Wang, and Q. Zhang, *J. Phys. Chem. B* 103 (1999) 5657.
- [28] C. Di Valentin, G. Pacchioni, M. Chiesa, E. Giamello, S. Abbet, and U. Heiz, *J. Phys. Chem. B* 106 (2002) 1637.
- [29] W. F. Schneider, K. C. Hass, M. Miletic, and J. L. Gland, *J. Phys. Chem. B* 106 (2002) 7405.
- [30] M. Sanders and J. H. Craig, *Thin Solid Films* 414 (2002) 251.

- [31] C. Bater, M. Sanders, and J. H. Craig, Jr., *Surf. Interface Anal.* 29 (2000) 188.
- [32] J. Lozano, J. H. Campbell, and J. H. Craig, Jr., *Appl. Surf. Sci.* 136 (1998) 159.
- [33] S. Ateca, C. Bater, M. Sanders, and J. H. Craig, Jr., *Surf. Interface Anal.* 29 (2000) 194.
- [34] Jose Lozano, Ph. D. dissertation, Univ. of Texas at El Paso (1998).
- [35] Chelon Bater, Ph. D. dissertation, Univ. of Texas at El Paso (1999).
- [36] Matthew Allen Sanders, Ph. D. dissertation, Univ. of Texas at El Paso (2000).
- [37] B. M. Davies and J. H. Craig, Jr., *Appl. Surf. Sci.* 205 (2003) 22.
- [38] M. J. Drinkwine and D. Lichtman, "Partial pressure analyzers and analysis," (American Vacuum Society, Monograph Series, 1978).

Figure Captions

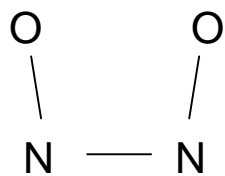
Fig. 1 (a) Structure of the gas-phase NO dimer. (b) One possible bonding geometry of the dimer on a surface. Other possible geometries include lying-down and inverted, oxygen-down orientations.

Fig. 2 TPD curves for various doses of N₂O on Ge(100) at 110 K, with no electron irradiation. Heating rate is 3 K/s.

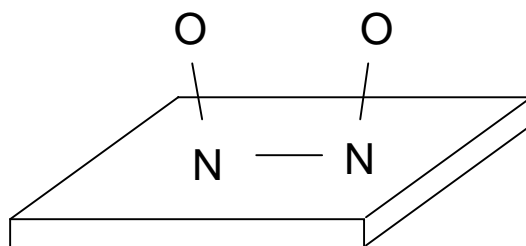
Fig. 3 Electron-stimulated desorption curves for various exposures of NO on Ge(100) at 110 K, obtained during a 2 min electron irradiation, with no heating.

Fig. 4 Electron-stimulated desorption curves for a 0.5 L dose of N₂O on Ge(100) at 110 K, obtained during a 10 min electron irradiation, with no heating.

Fig. 5 TPD curves for a 0.5 L dose of N₂O on Ge(100) at 110 K, after 10 min electron irradiation. Heating rate is 3 K/s.



(a) dimer molecule



(b) possible bonding geometry

Fig. 1

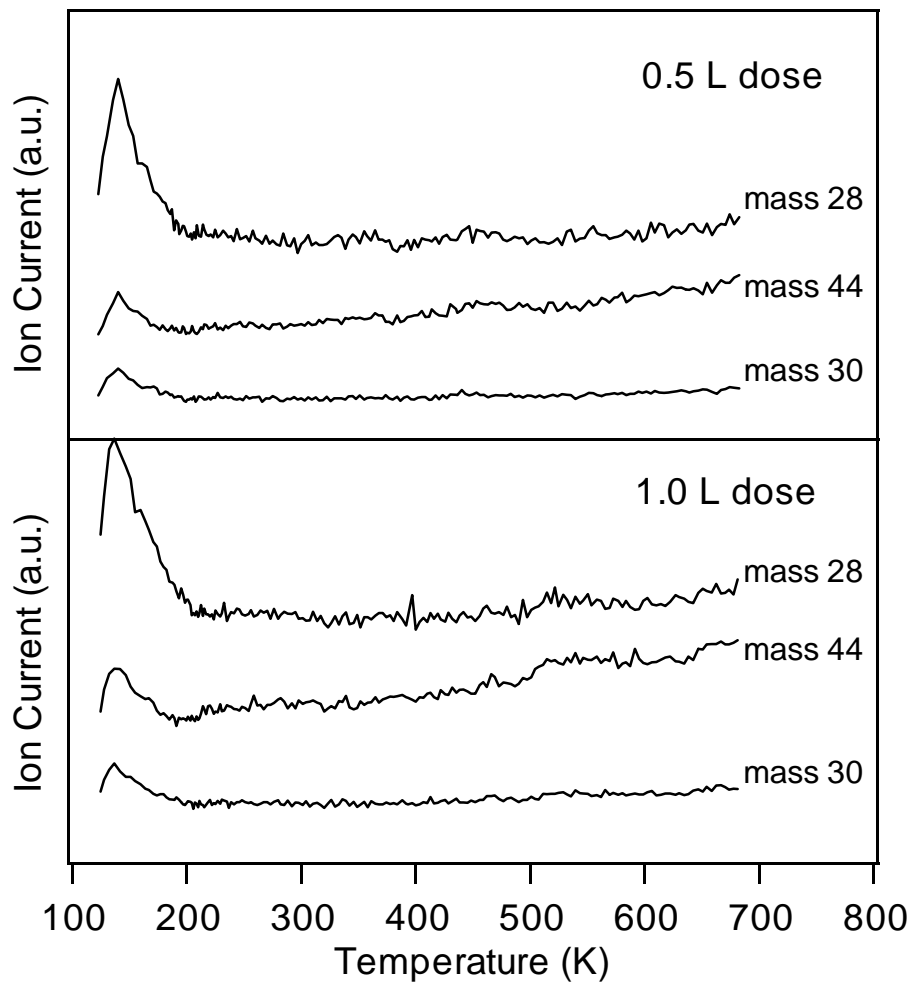


Fig. 2

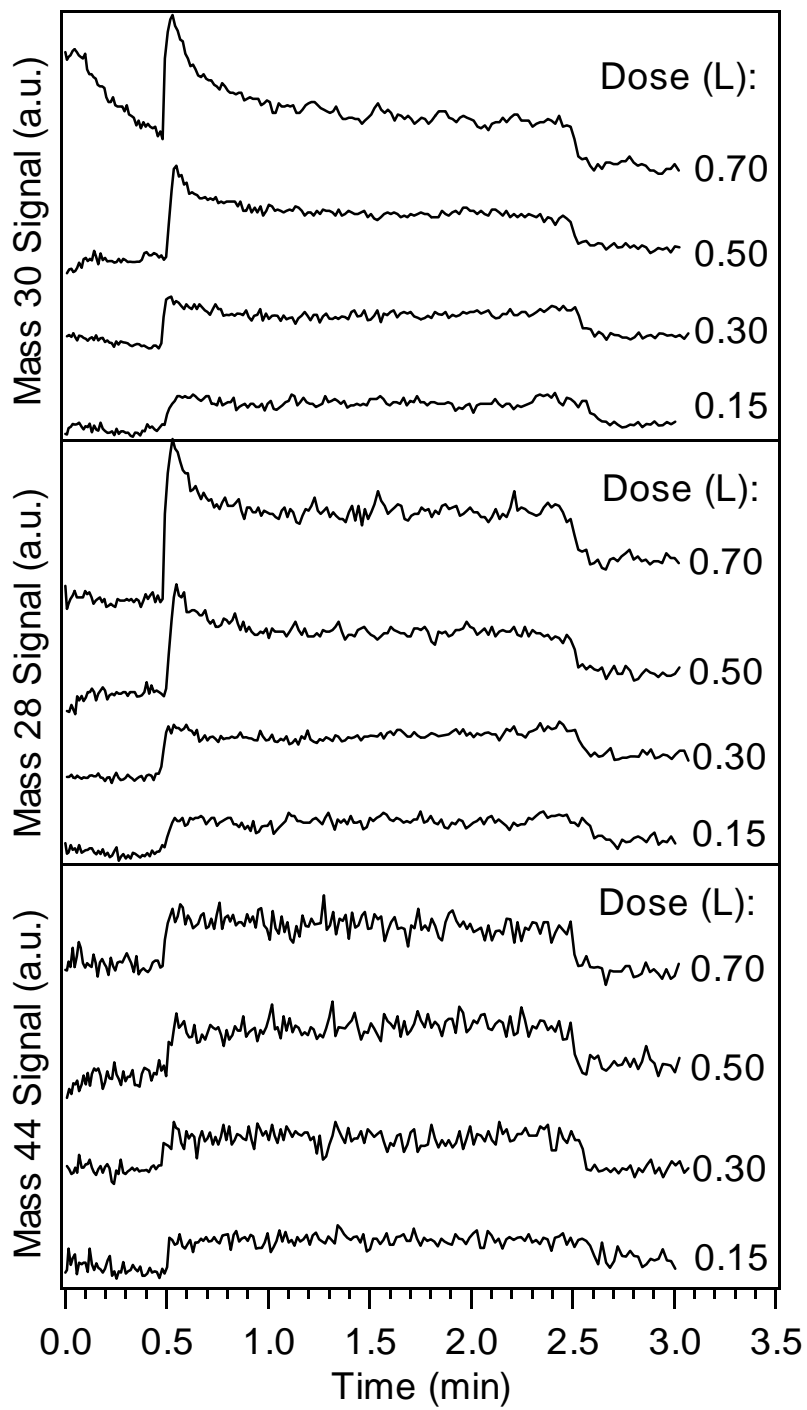


Fig. 3

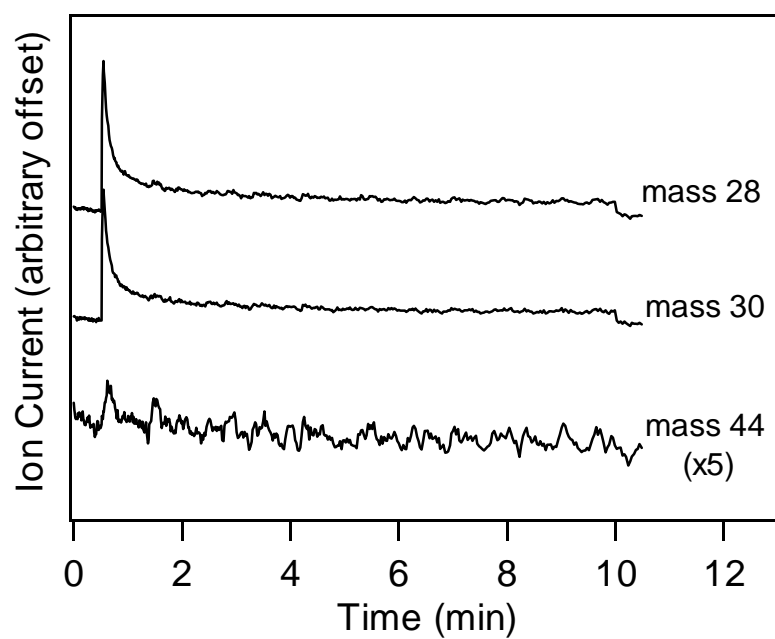


Fig. 4

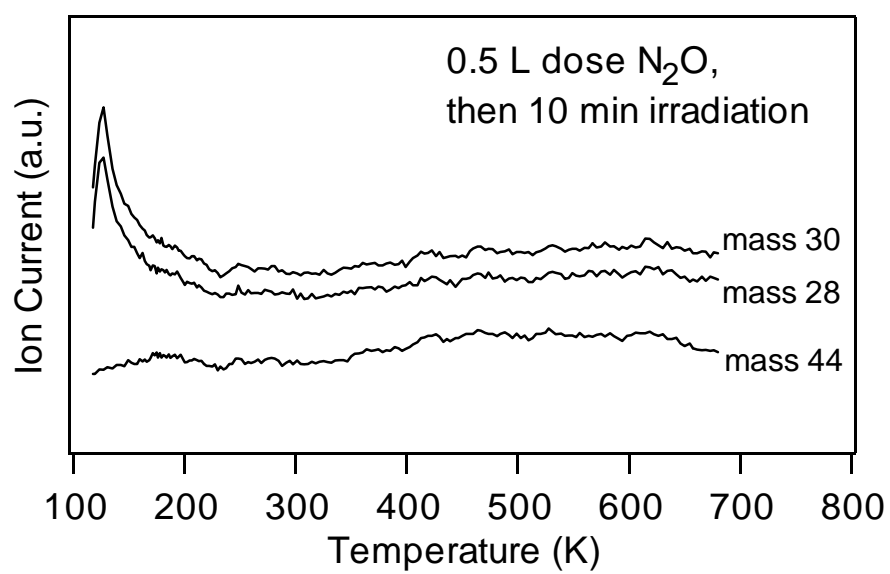


Fig. 5